Available online at www.sciencedirect.com
ScienceDirect
C. R. Physique 10 (2009) 70–82
COMPTES RENDUS PHYSIQUE

New approaches in Electromagnetic Compatibility / Nouvelles approches en Compatibilité Electromagnétique

# Use of the circuit approach to solve large EMC problems

Samuel Leman [a,*], Bernard Demoulin [a], Olivier Maurice [b], Michel Cauterman [c], Patrick Hoffmann [d]

[a] *Université des sciences et technologies de Lille, TELICE group IEMN, bâtiment P3, 59655 Villeneuve d'Ascq cedex, France*
[b] *GERAC, 3, avenue Jean-d'Alembert, ZAC de Pissaloup, 78190 Trappes, France*
[c] *Laboratoire des signaux et systèmes, CNRS-Supélec-Université Paris Sud 11, 91192 Gif-sur-Yvette cedex, France*
[d] *DGA, Centre d'étude de Gramat, 46500 Gramat, France*

Available online 17 March 2009

**Abstract**

Like electromagnetic topology, the equivalent electric circuit theory can be transposed to solve large electromagnetic systems. Compared to measures into a cavity, an analogy with coupled circuits will be made. Kron's formalism has been chosen to describe the system of equations. We will use a hyper matrix impedance with sub-matrix describing some interactions of the system. The inverse of the impedance matrix will give us scattering parameters $S_{21}$ between a transmitting and a receiving antenna installed in the cavity. Next, a second receiver will be added outside the cavity.

The aim of this article is to show the interest of Kron's method applied to complex systems, in which many of physical phenomena are involved. ***To cite this article: S. Leman et al., C. R. Physique 10 (2009).***


**Résumé**

**Utilisation de la théorie des circuits pour la CEM des grands systèmes.** Au même titre que la topologie électromagnétique, la théorie des circuits électriques peut être transposée pour la résolution de problèmes électromagnétiques complexes. En prenant pour base des expériences réalisées sur une cavité, nous allons procéder à une analogie avec des circuits couplés. Puis, à l'aide du formalisme de Kron, nous décrirons une super matrice impédance dans laquelle figurerons des sous-matrices révélatrices des différents couplages mis en jeu. L'inversion de cette matrice mènera finalement à la détermination du coefficient de transfert $S_{21}$ liant un monopole émetteur et un premier monopole récepteur installé dans cette cavité. Un second monopole récepteur sera ensuite mis en place à l'extérieur de la cavité.

L'objectif de cet article, est de mettre en évidence l'intérêt de la méthode de Kron appliquée à des systèmes complexes, c'est-à-dire, faisant intervenir de nombreux phénomènes physiques de différentes natures. ***Pour citer cet article : S. Leman et al., C. R. Physique 10 (2009).***


*Keywords:* Large EMC problems; Topology analysis; G. Kron's formalism; Tensorial analysis of electrical networks; *E.M*. cavity

*Mots-clés :* CEM des grands systèmes ; Analyse topologique ; Formalisme de G. Kron ; Analyse tensorielle des réseaux ; Cavité *E.M*

* Corresponding author.
*E-mail addresses:* s.leman@ed.univ-lille1.fr (S. Leman), bernard.demoulin@univ-lille1.fr (B. Demoulin), olivier.maurice@gerac.com (O. Maurice), Michel.Cauterman@lss.supelec.fr (M. Cauterman), patrick.hoffmann@dga.defense.gouv.fr (P. Hoffmann).

1631-0705/$ – see front matter 
doi:10.1016/j.crhy.2009.01.006

## 1. Introduction

More and more EMC engineers are concerned with the prediction of the disturbances occurring in various circuits of large electronic systems. A car or an aircraft affected by electromagnetic interference due to a radar beam or lightning are two typical examples where the determination of the current or voltage appearing at certain sensitive places of the circuit provides interesting guide lines about the characterization of EMC protection, such as the use of a filter, shield or ground connection topology. Such work may be achieved in several ways; the theoretical prediction by means of a full wave tool seems the most attractive. However, it requires a lot of computation time and memory storage, which are often incompatible when a few geometrical parameters or other parameters must be changed in order to know the variation gap in terms of EMC constraints probability.

For this reason, some alternative approaches avoiding computation steps with a full wave model were explored, such as the topology due to C. Baum [1] in 1980, tested and improved by J.P. Parmentier [2] ten years later, and more recently, the use of circuit assembly as proposed by O. Maurice [3]. This article is devoted to the last technique, where the various electromagnetic couplings provided in a large system will be reduced to the interaction between many equivalent circuits with the combination of inductance, capacitance and resistance joined with emf RF depending on the electromagnetic interference context. The main advantage of this methodology is for solving the circuit theory with the concepts of mesh and branch currents established by G. Kron [4,5] and leads to the construction of a hyper matrix impedance. Using the appropriate scale factor, each element of this matrix may be related to the electromagnetic coupling involved in a large system. From the computation of the inverse form of this matrix, the amplitude of disturbance in various location of the large system may be known. This tool allows one to keep the physical aspect of EM interactions in opposition to a classical 3D approach.

Section 2 of the paper gives a brief description of the system under consideration, which consists in the arrangement of monopoles coupled inside and outside a cavity. The aim of this test setup is to produce resonance in the cavity and combine with induction on short and long monopoles with respect to the wavelength.

Section 3 consists in the system description by means of a topological diagram as considered by the previous authors. From the graph facility we can deduce the ways of the main electromagnetic coupling which determine specified blocks in the equivalent circuit assembly.

After a short description of Kron's method in Section 4, Section 5 deals with the construction of the diagonal element attached to the hyper matrix impedance, neglecting electromagnetic coupling. This section is mainly focused on the conversion of the eigen modes appearing in the flat rectangular shaped cavity into RLC circuit resonators.

Section 6 is related to the final filling of the hyper matrix by the coefficient and sub-matrices involving the electromagnetic coupling.

In Sections 7 and 8, we will propose a comparison between experiments and simulations performed as described above and some conclusions will be added about the expected application of this method on an industrial scale.

## 2. System under consideration

Fig. 1 shows a short description of the system to be solved with the so-called circuit approach. It consists of two short monopole antennas coupled inside a rectangular shaped cavity. Monopole 1 is connected to an RF source, while the short monopole 2, used as a receiving antenna, forms directly a junction with a long monopole coming out of the cavity. A similar monopole placed at distance $d_{12}$ of about 9 cm from the previous one will be connected to a receiver as a network analyzer. We can mention that the height $h$ of the short monopole inside the cavity will be chosen very small with respect to the wavelength ($h \ll \lambda$); then the length of the monopoles 2 and 3 outside are $h_2 = h_3 = 19$ cm in order to reach the resonance condition of these wires.

The height $c$ of the box will be very small compared to the wavelength explored in order to behave like a 2D cavity. To study theory and measurements within the frequency range 100 MHz to 2 GHz, we suggest using the following dimensions $a = 42$ cm, $b = 28$ cm and $c = 3.8$ cm for this cavity. According to the Cartesian axis $Oxyz$ in Fig. 1, we can notice that the exact locations of the monopoles inside the cavity expressed in centimeters will be $(x_0, y_0) = (21; 14)$ for monopole 1, $(x, y) = (21; 21)$ for monopole 2 and $(x, y) = (21; 30)$ for monopole 3.

The next step will be devoted to the characterization of the $S_{21}$ parameter relevant to the electromagnetic coupling throughout monopole 1 and 3, especially to detecting the combination of resonance phenomena occurring inside the cavity and at the level of the monopole 2 coming out of the cavity, with monopole 3 used as a receiving wire. General

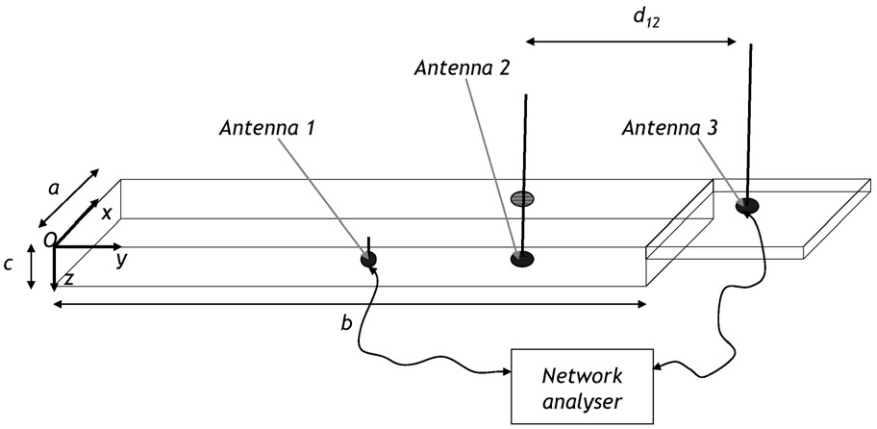


Fig. 1. Description of the test setup.

theory of the empty rectangular shaped cavity shows that the eigen modes occur with frequencies $f_{\text{mnp}}$ given by the following formula:

$$f_{\text{mnp}} = \frac{v}{2}\sqrt{\left(\frac{m}{a}\right)^2 + \left(\frac{n}{b}\right)^2 + \left(\frac{p}{c}\right)^2} \tag{1}$$

According to the dimensions mentioned $a, b, c$, the first eigen mode of this cavity will be given for $n = 0, m = 0$ and $p = 1$, which corresponds to a frequency of 3.95 GHz.

$$f_{0,0,1} = \frac{v}{2}\sqrt{\left(\frac{1}{c}\right)^2} = 3.95 \text{ GHz} \tag{2}$$

As suggested above, the depth $c$ of the cavity is very small compared to the wavelength in order to give it a 2D behavior with frequencies just below 3.95 GHz. For this reason the maximum value of the frequency explored will be 2 GHz in order to consider only the contribution of degenerated modes forcing the parameter $p$ to zero.

## 3. Sub-network arrangement of the problem

The preliminary work will be to produce a topological graph of the system to extract the arrangement of several sub-networks which may be easier to convert into electrical circuits for the final use.

From the electromagnetic coupling point of view, we can recognize five sub-networks with the following encoded topological volumes. The transmitting short monopole 1 inside the cavity corresponds to the volume $V_{3,1}$, while the empty cavity itself will be noted by the volume $V_{3,2}$. Part of the receiving monopole 2 inside the cavity consists of the volume $V_{3,3}$, then the outer part of this monopole forms the volume $V_{3,4}$. At this level of topological description, we find the monopole 3 connected to the receiver, which forms the volume $V_{3,5}$. Consequently, a brief analysis of the topological graph in Fig. 2 from bottom to top shows that the link between $V_{3,1}$, $V_{3,2}$ and $V_{3,3}$ leads to the volume $V_{2,1}$ which includes the coupling phenomena within the cavity, and the link between $V_{3,4}$ and $V_{3,5}$ is related to the coupling outside the cavity noted volume $V_{2,2}$. Finally, joining the previous volumes $V_{2,1}$ and $V_{2,2}$ links all coupling of the large system attached with the topological volume $V_{1,1}$.

The aim of the proposed approach will be to reduce each sub-network to a circuit composed of the arrangement of inductance, capacitance, resistance with voltage or current source; each is specified by the type of electromagnetic coupling occurring in layer 3 of the topological diagram. Thus Fig. 3 shows one example of conversion in terms of equivalent electrical circuits. This representation has been chosen for testing the efficiency of equivalent electrical model of cavities.

According to Kron's methodology, it requires the combination of "mesh" network and "branch" network. Thus the diagram on the left corresponds to the mesh network involving the emf $e$ and inner 50 Ω resistance $R_0$ of the RF source connected at monopole 1 and forming the previously mentioned volume $V_{3,1}$. Just on the right, we find amount

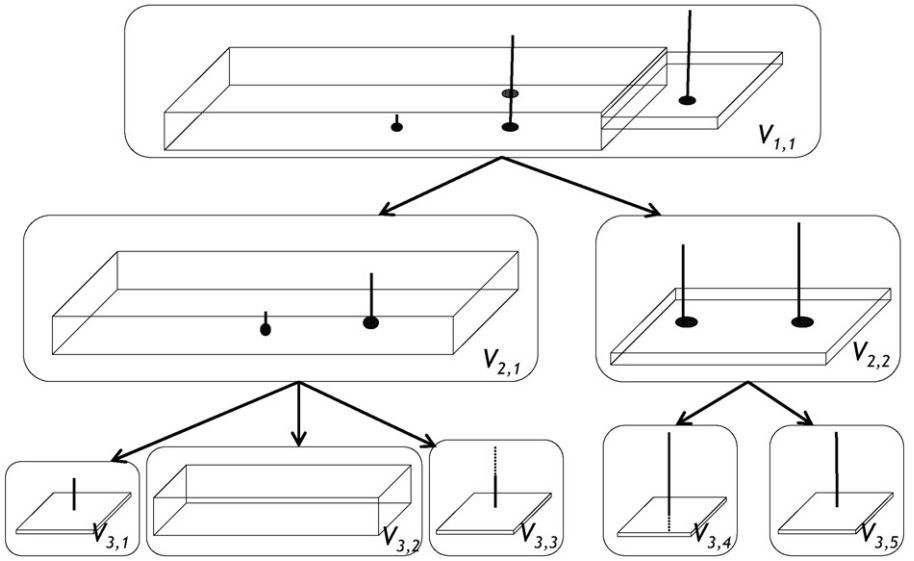


Fig. 2. Topology diagram of the test setup.

of $R, L, C$ resonators to convert the empty cavity attached to the volume $V_{3,2}$ into circuit elements. Details about the constitution of these elements will be brought in Eqs. (5)–(9). Volume $V_{3,3}$, related to the monopole 2, especially its short part placed inside the cavity is assumed to be a simple mesh network with the resistance $R_2$ which corresponds to the 50 Ω termination between this wire and the bottom face of the cavity. Volume $V_{3,4}$ attached to the upper part of monopole 2 outside the cavity is focused towards a mesh network including inner impedance $Z_{\text{ant22}}$ of this monopole and 50 Ω termination. We can notice that when the wavelength becomes short with respect to this monopole, the value of $Z_{\text{ant22}}$ may change strongly with frequency. As previously mentioned, volume $V_{3,5}$ attached with the long monopole 3 is related to the mesh network where $Z_{\text{ant3}}$ and $R_3$ correspond to its inner impedance and the 50 Ω load input impedance of the receiver, respectively.

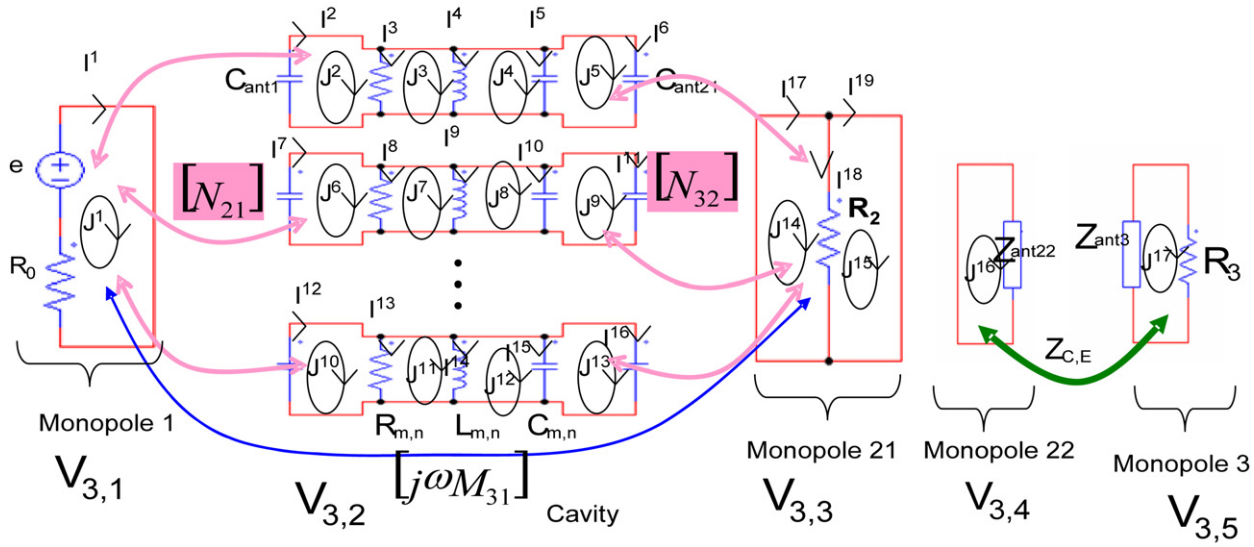


Fig. 3. Circuit diagram of the test setup.

Various links between the topological volumes in layer 3 are established by the parameters of Fig. 3 related to the coupling phenomena. Coefficients $N_{21}$ and $N_{32}$ are defined by two matrices involving the field pattern through

the $Oxy$ plane of the cavity; details about these will be given afterwards. Direct coupling between the transmitting monopole 1 and short part of monopole 2 is summarized by $j\omega M_{31}$ which is similar to induced voltages at both sides of volume $V_{3,1}$ and $V_{3,3}$. Since the distance between these short antennas may be similar to the wavelength, $M_{31}$ depends on the frequency; to avoid any numerical computation, this coefficient will be directly deduced from measurements carried out with a network analyzer. Furthermore, according to the fact that the height of monopole 1 and short part of monopole 2 are smaller than the wavelength, they behave like small capacitances $C_{\text{ant1}}$ and $C_{\text{ant21}}$. For convenience sake, we can notice in Fig. 3 that they are placed at both sides of each $R, L, C$ resonator. The link between volumes $V_{3,3}$ and $V_{3,4}$ needs the continuation of the current when the wire of monopole 2 is crossing the upper side of the cavity, then volumes $V_{3,4}$ and $V_{3,5}$ are connected by means of $Z_{CE}$ mutual impedance. As previously, this parameter is provided from measurements; additional details about the coupling throughout the topological volumes will be brought in Section 5 of the paper.

## 4. Solving the problem with the circuit approach by means of Kron's methodology

According to the diagram in Fig. 3 each part of the circuit may be characterized in terms of mesh current with attached contravariant tensor $J^i$ and branch current with attached contravariant tensor $I^i$. The relationship between mesh current and branch current is given by the condition involved at each node of the circuit and contained in vector. In a similar way, the various voltage sources installed on the branches of these circuits are related to a covariant vector $E_i$ which forms an emf vector. From the topology of the circuit like the diagram in Fig. 3, we can find a relation between the emf vector and the mesh current vector:

$$[E] = [Z][J] \tag{3}$$

As a general rule, the mesh current vector is unknown; then after construction of the matrix $[Z]$ taking into account the circuit topology in Fig. 3, we can deduce from the inverse product the $[J]$ vector and consequently the response at various points of the circuit.

From the theoretical point of view, the main restriction of Kron's method deals with propagation phenomena which require that the circuit must be formed with lumped elements.

The next section of the paper will be devoted, step by step, to the determination of each parameter of matrix $[Z]$, the so-called hyper matrix impedance of the large system.

## 5. Construction of the hyper matrix [Z] without the electromagnetic coupling

From the diagram in Fig. 3, we can deduce a preliminary arrangement of the hyper matrix neglecting electromagnetic interaction, as shown in Eq. (4): it consists of a diagonal with parameters composed of sub-matrix $[Z_k]$ related to the corresponding volume in layer 3 of the topological diagram in Fig. 2. The determination of these sub-coefficients is given simply according to Kron's method exposed in previous section.

$$E = \begin{bmatrix} [E_1] \\ [E_2] \\ [E_3] \\ [E_4] \\ [E_5] \end{bmatrix}, \qquad Z = \begin{bmatrix} [Z_1] & [0] & [0] & [0] & [0] \\ [0] & [Z_2] & [0] & [0] & [0] \\ [0] & [0] & [Z_3] & [0] & [0] \\ [0] & [0] & [0] & [Z_4] & [0] \\ [0] & [0] & [0] & [0] & [Z_5] \end{bmatrix} \tag{4}$$

Thus the matrix $[Z_1]$ is reduced to the scalar $R_0$, while according to the relationship between the mesh current in $V_{3,3}$, the matrix $[Z_3]$ given by Eq. (5) may be established since the branches of this circuits do not include emf sources. This shows that the right-hand side of the equation is cancelled.

$$\begin{aligned} J^{14}R_2 - J^{15}R_2 &= 0 \\ -J^{14}R_2 + J^{15}R_2 &= 0 \end{aligned} \tag{5}$$

Consequently, the size in matrix $[Z_3]$ is given by the number of mesh involved in volume $V_{3,3}$, while the subscripts of the mesh current vector are encoded in respect of the size of matrix $[Z_1]$ and $[Z_2]$ respectively. From these rules, matrix $[Z_4]$ and $[Z_5]$ will be found in a similar way:

$$Z_1 = [R_0], \qquad Z_3 = \begin{bmatrix} R_2 & -R_2 \\ -R_2 & R_2 \end{bmatrix}$$
$$Z_4 = [Z_{\text{ant22}}], \qquad Z_5 = [R_3 + Z_{\text{ant3}}] \tag{6}$$

Extending this approach to the determination of the sub-matrix $[Z_2]$ related to an $N$ resonator arrangement requires a recall of the electromagnetic theory of cavities. As shown in a recent work published by M. Cauterman [6,7], the electromagnetic response of a 2D cavity excited by a line source may be easily simulated by the arrangement of $R, L, C$ resonators. We recall that a 2D cavity consists of an infinite long tube with uniform cross section. When it has a rectangular shape, the 2D is similar to the usual infinitely long wave guide; as briefly shown hereafter, a 3D flat rectangular cavity working below its first eigen mode behaves like a 2D model.

As a general rule, a 3D cavity may be solved from the Helmholtz equation (7), where $E_z$ deals with the electric field component collinear to the $z$ axis parallel to the small dimension $c$ of the rectangular box as described in Fig. 1. The right side of this equation includes the Dirac function, which is related to the transmitting antenna placed inside the cavity. Assuming this antenna to be similar to a Hertzian dipole, the right term is cancelled except at the location of the antenna.

$$\left[\frac{\partial^2}{\partial x^2} + \frac{\partial^2}{\partial y^2} + \frac{\partial^2}{\partial z^2} + k^2\right] E_Z = j\omega\mu I_0 \delta(r - r') \tag{7}$$

In a standard way, Eq. (7) may be solved and lead to Eq. (8) where the values assigned with the coefficients $\varepsilon_{0m}, \varepsilon_{0n}, \varepsilon_{0p}$ are selected in respect of the mode configurations [8].

$$\begin{aligned}\vec{E}_z(x,y,z) = {} & \frac{\varepsilon_{0n}.\varepsilon_{0m}.\varepsilon_{0p} j\omega\mu_0 I_0 h_{\text{ant}}}{k^2 abc} \sum_{m=1}^{\infty}\sum_{n=1}^{\infty}\sum_{p=0}^{\infty} \frac{1}{k^2 - (m\pi/a)^2 - (n\pi/b)^2 - (p\pi/c)^2} \\ & \times \left\{\left[\left(\frac{m\pi}{a}\right)^2 + \left(\frac{n\pi}{b}\right)^2\right] \sin(m\pi x_0/a)\sin(m\pi x/a)\sin(n\pi y_0/b)\sin(n\pi y/b)\cos(p\pi z_0/c)\cos(p\pi z/c)\vec{z}\right. \\ & - \frac{n\pi}{b}\left(\frac{p\pi}{c}\right)\sin(m\pi x_0/a)\sin(m\pi x/a)\cos(n\pi y_0/b)\sin(n\pi y/b)\sin(p\pi z_0/c)\cos(p\pi z/c)\vec{y} \\ & \left. - \frac{m\pi}{a}\left(\frac{p\pi}{c}\right)\cos(m\pi x_0/a)\sin(m\pi x/a)\sin(n\pi y_0/b)\sin(n\pi y/b)\sin(p\pi z_0/c)\cos(p\pi z/c)\vec{x}\right\}\end{aligned} \tag{8}$$

As recalled in Eq. (2) the first eigen mode of the 3D cavity is given by the minimum value of the frequency $f_{\text{mnp}}$ where transverse magnetic components $H_x$ and $H_y$ and electric components $E_x$ and $E_y$ do not vanish for the *TE* modes and *TM* modes, respectively. According to the dimensions specified in Section 2 this occurs for $p = 1, m = 0$ and $n = 0$, which correspond to the frequency of 3.95 GHz. Otherwise especially for $p = 0$, the mode configurations leading to the value of $f_{\text{mnp}}$ below 3.95 MHz are similar to those found for a 2D rectangular shaped cavity. Then $E_z$ electric field component attached with the *TM* mode behaves like the restricted form of Eq. (8):

$$E_Z = \frac{4 j\omega\mu_0 I_0 h_{\text{ant}}}{abc} \sum_{m=1}^{\infty}\sum_{n=1}^{\infty} \frac{\sin(m\pi x_0/a)\sin(m\pi x/a)\sin(n\pi y_0/b)\sin(n\pi y/b)}{k^2 - (m\pi/a)^2 - (n\pi/b)^2} \tag{9}$$

To match Eq. (9) with the circuit concept, a scale factor $\alpha$ will be considered to transform $E_z$ electric field amplitude into voltage amplitude *V*. For this reason Eq. (9) can be rewritten as in Eq. (10):

$$V = \alpha E_z \rightarrow V = \sum_{n=1}^{\infty}\sum_{m=1}^{\infty} \frac{N_{mn} N'_{mn} j L_{mn}\omega}{1 - \omega^2/\omega_{mn}^2} I_0 \tag{10}$$

In Eq. (10) appears the parameter $N_{mn}$ related to the coupling between the monopole 1 and the 2D $TM_{mn}$ according to Eq. (11) involving the sinusoidal function at the numerator of Eq. (9); in the same way, we deduce $N'_{mn}$ related to the coupling between $TM_{mn}$ and the $E_z$ component acting on the short part of monopole 2 inside the cavity:

$$N_{mn} = \sin\left(m\frac{\pi x_0}{a}\right)\sin\left(n\frac{\pi y_0}{b}\right), \qquad N'_{mn} = \sin\left(m\frac{\pi x}{a}\right)\sin\left(n\frac{\pi y}{b}\right) \tag{11}$$

In Eq. (11), we find the angular frequency $\omega_{mn}$ attached to $a$ and $b$, the dimensions of the box:

$$\omega_{mn} = 2\pi f_{mn} \quad \text{with } f_{mn} = \frac{v}{2}\sqrt{\left(\frac{m}{a}\right)^2 + \left(\frac{n}{b}\right)^2} \tag{12}$$

Another parameter found in the voltage equation (10) deals with the inductance $L_{mn}$ attached with $TM_{mn}$ it may be deduced by equalizing $E_z$ from Eqs. (9) and (10). Furthermore, the use of the resonator circuit as shown in diagram of Fig. 3 involves the capacitance $C_{mn}$ which may be easily deduced from the well known relationship between $\omega_{mn}$ and its corresponding inductance and capacitance:

$$L_{mn} = \frac{4\mu_0 h_{\text{ant1}}\alpha}{abck_{mn}^2} \quad \text{with } \omega_{mn} = \frac{1}{\sqrt{L_{mn}C_{mn}}} \rightarrow C_{mn} = \varepsilon_0 \frac{abc}{4h_{\text{ant1}}\alpha} \tag{13}$$

The previous computation assumed a perfect empty cavity without losses, in order to take into account the dissipated thermal power in the walls of the box with high electric conductivity $\sigma$. Eq. (10) may be somewhat changed with the insertion of the $Q$ factor attached to the $TM_{mn}$ mode as follow:

$$V = \sum_{n=1}^{\infty}\sum_{m=1}^{\infty} \frac{N_{mn}N'_{mn}jL_{mn}\omega}{1-(\omega^2/\omega_{mn}^2)(1-j/Q_{mn})} I_0 \quad \text{with } Q_{mn} = R_{mn}C_{mn}\omega \tag{14}$$

In Eq. (14) the value of the $Q$ factor may be deduced from the 3D model with $p = 0$ according to Eq. (15) below, where the skin depth $\delta$ in the high conductive material appears. We can notice that the losses in the system depicted in Fig. 1 are mainly due to the thermal effect in the 50 Ω termination of monopole 2 and the inner resistance of the RF source.

$$\begin{aligned} Q_{mn} &= \frac{\eta abck_{0mn}(k_x^2 + k_y^2)}{2R_w[b(a+c)k_x^2 + a(b+c)k_y^2]} \\ k_x &= \frac{m\pi}{a}, \quad k_y = \frac{n\pi}{b}, \quad k_{mn} = \sqrt{k_x^2 + k_y^2}, \quad R_w = \frac{1}{\sigma\delta} \end{aligned} \tag{15}$$

Computation of these formulas for the 2D lower resonance frequency leads to the following values for the first resonator appearing in Fig. 3.

$$f_{1,1,0} = 646\ \text{MHz}, \quad L_{11} = 0.93\ \text{nH}, \quad C_{mn} = 65.5\ \text{pF}, \quad R_{11} = 47\ \text{k}\Omega, \quad N_{11} = 1, \quad N'_{11} = 0.705 \tag{16}$$

Usually the resonator attached with the 2D $TM_{mn}$ mode may be presented with the diagram in Fig. 4 and its branch current noted $I^k$ where the top subscript $k$ is related to the $k$th branch of the circuit. In Fig. 4 we consider the contribution of five branches with 3, 4 and 5 corresponding to the resistance $R_{mn}$, inductance $L_{mn}$ and capacitance $C_{mn}$ related to $TM_{mn}$. At both sides of this circuit the coupled capacitance with monopoles 1 and 2 have been added on each resonator, they are concerned by branch currents $I^2$ and $I^6$.

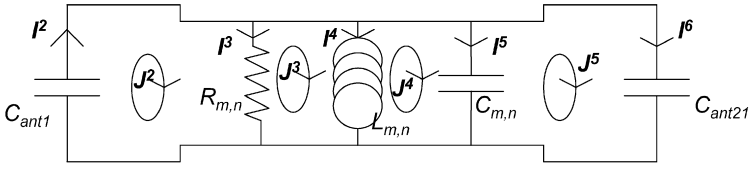


Fig. 4. Branch currents and mesh currents attached to one RLC resonator.

For convenience's sake the diagram in Fig. 4 may be transformed into a product of matrix involving the voltage vector $[V_{mn}]$, the branch current vector $[I_{mn}]$ and the branch impedance matrix $[Z_{mn}]$ as written below:

$$[V_{mn}] = [Z_{mn}][I_{mn}] \tag{17}$$

Details about the full diagonal impedance matrix expressed in terms of branch currents for each resonator are given in Eq. (18).

$$Z_{mn} = \begin{bmatrix} \frac{1}{j\omega C_{\text{ant1}}} & 0 & 0 & 0 & 0 \\ 0 & R_{mn} & 0 & 0 & 0 \\ 0 & 0 & j\omega L_{mn} & 0 & 0 \\ 0 & 0 & 0 & \frac{1}{j\omega C_{mn}} & 0 \\ 0 & 0 & 0 & 0 & \frac{1}{j\omega C_{\text{ant21}}} \end{bmatrix} \tag{18}$$

We can mention that the value of the capacitances related to monopole 1 and the short part of monopole 2 inside the box are deduced from the usual analytical formula in Eq. (19), the heights $h_1$ and $h_2$ of these short antennas are 1 cm and 2 cm respectively, while the wires diameters are about $d = 1.5$ mm each.

$$C_{\text{ant}} = \frac{2\pi\varepsilon_0}{\ln(4h/d)}h, \quad C_{\text{ant1}} = 0.18 \text{ pF}, \quad C_{\text{ant21}} = 0.28 \text{ pF} \tag{19}$$

However, to include this matrix in the above Eq. (3), one additional computation is required in order to change the branch current into mesh current by means of the commutation matrix $[L]$ as found in Eq. (20).

$$\begin{aligned} I^2 &= J^2 + 0J^3 + 0J^4 + 0J^5, \\ I^3 &= J^2 - J^3 + 0J^4 + 0J^5, \\ I^4 &= 0J^2 + J^3 - J^4 + 0J^5, \\ I^5 &= 0J^2 + 0J^3 + J^4 - J^5, \\ I^6 &= 0J^2 + 0J^3 + 0J^4 + 1J^5, \end{aligned} \qquad L = \begin{bmatrix} 1 & 0 & 0 & 0 \\ 1 & -1 & 0 & 0 \\ 0 & 1 & -1 & 0 \\ 0 & 0 & 1 & -1 \\ 0 & 0 & 0 & 1 \end{bmatrix} \tag{20}$$

Consequently each coefficient of the matrix in the mesh configuration may be written by using Einstein notation:

$$Z'_{n_{b\beta}} = L^a_b Z_{n_{ac}} L^c_\beta; \quad a, b, c, \beta = 1, 2, \ldots, r \tag{21}$$

According to the fact that the number of resonators considered with the diagram in Fig. 3 depends of the location of the 3D first eigen mode in respect of the first 2D resonance frequency, the sums in Eqs. (10) and (14) will be restricted to $N$ modes appearing within this frequency range. Then matrix $[Z_2]$ in Eq. (3) can be written according to the full diagonal form of size $N$:

$$Z_2 = \begin{bmatrix} [Z'_1] & 0 & 0 & 0 \\ 0 & [Z'_2] & 0 & \ldots \\ 0 & 0 & \ldots & 0 \\ 0 & \ldots & 0 & [Z'_i] \end{bmatrix} \tag{22}$$

Each element of matrix $[Z_2]$ may be easily deduced from Eq. (22) and filled as shown in Eq. (23).

$$Z'_i = \begin{bmatrix} \frac{1}{j\omega C_{\text{ant1}}} + R_{mn} & -R_{mn} & 0 & 0 \\ -R_{mn} & R + j\omega L_{mn} & -j\omega L_{mn} & 0 \\ 0 & -j\omega L_{mn} & j\omega L_{mn} + \frac{1}{j\omega C_{mn}} & -\frac{1}{j\omega C_{mn}} \\ 0 & 0 & -\frac{1}{j\omega C_{mn}} & \frac{1}{j\omega C_{mn}} + \frac{1}{j\omega C_{\text{ant21}}} \end{bmatrix} \tag{23}$$

Before concluding this section, we will make some comments about the scale factor $\alpha$ introduced in Eq. (10). As mentioned above, this factor links electric field data found at both sides of the cavity and voltage data appearing with the circuit diagram in Fig. 3. Since the physical unit of $\alpha$ is expressed in meters, the best way to determine this factor will be to use the relationship between $E_z$ and the emf induced on the short part of monopole 2 inside the box. Since this wire is loaded by 50 Ω and shortened with respect to the wavelength, $\alpha$ may be considered with 3.8 cm unit.

## 6. Insertion of electromagnetic coupling parameters in the circuit approach

In order to find the hyper matrix related to the whole circuit in Fig. 3, diagonal off element in Eq. (3) must be filled with additional scalar coefficient or sub-matrices involving various type of electromagnetic coupling.

Let us consider the connection between the short and outer part of monopole 2 which characterize the coupling between the topological volumes $V_{3,3}$ and $V_{3,4}$ as shown in Figs. 3 and 5. Mesh currents as presented on the left of

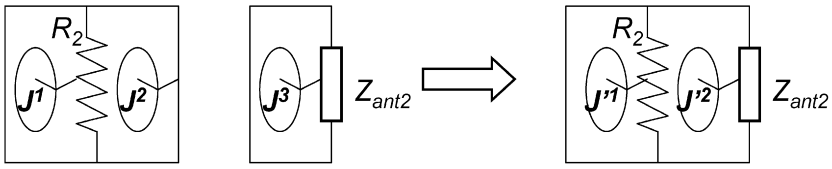


Fig. 5. Combination of topological volumes $V_{3,3}$ et $V_{3,4}$ by the cross connection matrix.

this figure with two separate meshes may be merged with one mesh only according to the use of the diagram on the right hand and the new mesh current noted here $J'$ and related to initial mesh current $J$ by Eq. (24).

$$\begin{aligned} J^1 &= 1.J'^1 + 0.J'^2 \\ J^2 &= 0.J'^1 + 1.J'^2 \\ J^3 &= 0.J'^1 + 1.J'^2 \end{aligned} \tag{24}$$

This equation consists of a linear transformation characterized by the so-called cross connection matrix $[F]$ as written in Eq. (25) and filled with parameters in Eq. (26).

$$[J] = [F][J'] \tag{25}$$

$$[F] = \begin{bmatrix} 1 & 0 \\ 0 & 1 \\ 0 & 1 \end{bmatrix} \tag{26}$$

Then the size of the initial hyper matrix $[Z]$ as given by Eq. (3) may be reduced by using the cross connection matrix:

$$[Z'] = [F]^t \begin{bmatrix} [Z_3] & 0 \\ 0 & [Z_4] \end{bmatrix} [F] \tag{27}$$

In this equation we find the transposed form of $[F]$, while the new matrix is noted $[Z']$, in the same way, part of emf vector $[E]$ dealing with $[E_3]$ and $[E_4]$ may be reduced according to the following:

$$[E'] = [F]^t \begin{bmatrix} [E_3] \\ [E_4] \end{bmatrix} \tag{28}$$

At last, Eq. (3) with size 5 behaves like Eq. (29) with size 4.

$$E = \begin{bmatrix} [E_1] \\ [E_2] \\ [E'] \\ [E_5] \end{bmatrix}, \qquad Z = \begin{bmatrix} [Z_1] & [0] & [0] & [0] \\ [0] & [Z_2] & [0] & [0] \\ [0] & [0] & [Z'] & [0] \\ [0] & [0] & [0] & [Z_5] \end{bmatrix} \tag{29}$$

The coupling between volumes $V_{3,1}$ and $V_{3,3}$ as shown in Fig. 3 involves the resonance occurring at the cavity level and direct coupling phenomena between monopole 1 and monopole 2. The first one may be characterized in terms of coupling parameters $N_{mn}$ and $N'_{mn}$ as mentioned in the analytical formula in Eq. (11).

Extending the circuit concept towards these coupling factors forms two full diagonal sub-matrices $[Z_{12}]$ and $[Z_{21}]$ where each coefficient is expressed in terms of the product between $N_{mn}$ and a scale factor $\beta$; it characterizes the coupling between the voltage source and each resonator. In the same way, the $N'_{mn}$ coefficients will be inserted in matrices $[Z_{23}]$ and $[Z_{32}]$ to characterize the coupling between the resonator and current amplitude induced in monopole 2. To find the scale factor $\beta$, we consider the transfer of electromagnetic energy within the mode $TM_{mn}$ i.e. the amplitude of $E_{zmn}$ electric field and the corresponding voltage $V_{mn}$ in the block diagram in Fig. 3. Regarding the topological volume $V_{3,1}$ the RF voltage source with emf $e$ produces the current $I^1$ given in Eq. (30).

$$I^1 = \frac{e}{R_0 + Z_{e1}} \tag{30}$$

In this formula, $R_0$ is the inner résistance of the voltage source, while $Z_{e1}$ forms the input impedance offered by the short monopole 1. According to the fact that the height $h_1$ of the monopole is very short compared to the wavelength, $Z_{e1}$ is provided by a capacitance of about 0.2 pF which is ten times less than the 2.4 pF of the coaxial $N$

connector receiving this small antenna, consequently $Z_{e1}$ written in Eq. (31), where $C_N$ is the concerned $N$ connector capacitance. In the considered frequency range going from 100 MHz to 2 GHz, fifty Ohms $R_0$ remains far below $Z_{e1}$ and $\beta$ may be expressed as written in Eq. (32).

$$R_0 \ll \frac{1}{C_N \omega} \rightarrow Z_{e1} \cong \frac{1}{jC_N\omega} \tag{31}$$

$$e = \beta I^1 \rightarrow \beta \cong \frac{1}{jC_N\omega} \tag{32}$$

The previous coupling impedances were related to the energy of one mode, but it is also a so-called additional direct coupling which concerns resonance outside the box and the electromagnetic interaction within monopoles 1 and 2. It occurs rather in the low frequency range, i.e. below the first 2D resonance and between two consecutive modes. It consists of two diagonal off coefficients $j\omega M_{13}$ and $j\omega M_{31}$ placed in location 3 in line 1 and location 3 in column 1 of the hyper matrix. They are similar to the mutual inductances. However, taking into account the fact that the distance between monopole 1 and monopole 2 may be similar to the wavelength, values of $M_{13}$ and $M_{31}$ may be moved with the frequency. For instance these coefficients will be deduced from measurements. The last diagonal off parameters found in this hyper matrix deal with the coupling between outer part of monopole 2 and monopole 3 connected to the receiver. It concerns the coupling between the volumes $V_{3,4}$ and $V_{3,5}$ of the topological diagram by means of the coupling impedance $Z_{CE}$, as previously deduced from measurements with a network analyzer. We can notice that in low frequency range a good approximation with $M_{13}$ and $M_{31}$ may be the value of 5 pH with 3.8 cm height $c$ of the box and 9 pH when it rises to 7.8 cm. The last step will be to add the diagonal off parameters in Eq. (33) which forms the final hyper matrix impedance, as shown in Eq. (34).

$$E = \begin{bmatrix} [E_1] \\ [E_2] \\ [E'] \\ [E_5] \end{bmatrix}, \qquad Z = \begin{bmatrix} [Z_1] & [\frac{N_{12}}{j\omega C_N}] & [j\omega.M_{13}] & [0] \\ [\frac{N_{21}}{j\omega C_N}] & [Z_2] & [\frac{N_{23}}{j\omega C_N}] & [0] \\ [j\omega.M_{31}] & [\frac{N_{32}}{j\omega C_N}] & [Z'] & [Z_{C,E}] \\ [0] & [0] & [Z_{C,E}] & [Z_5] \end{bmatrix} \tag{33}$$

We can deduce the mesh current in term of vector $[J]$ from the product on the right involving the emf vector $[E]$ and the computation of inverse hyper impedance matrix as written in Eq. (34).

$$[J] = [Z]^{-1} \cdot [E] \tag{34}$$

From the circuit approach of electromagnetic coupling, numerical data of scattered parameters will be compared to the measurements in next section of the paper.

## 7. Computation of $S_{21}$ parameters compared with measurements

Two configurations of the system in Fig. 1 will be tested. One is related to the determination of $S_{21}$ parameter between the input port of monopole 1 and the termination of the short part in monopole 2 placed at the back side of the cavity. The second concerns the determination of $S_{21}$ between the input port of the monopole 1 and the termination of the long monopole 3 placed outside the cavity.

The first tests will be performed with 3.8 cm and 7.8 cm for the height $c$ of the box. We can notice that for this two values of $c$, $h_1 = 1$ cm and $h_2 = 2$ cm. Computation of $S_{21}$ from the circuit approach as described in the previous sections uses Eq. (35) where $E_0$ corresponds to the emf of the sinusoidal wave source instead of the output port of the network analyzer, then $V_c$ is the voltage collected at monopole 2 output loaded with 50 Ω. We recall that the amplitude of $V_c$ may be easily deduced from the computation of the corresponding mesh current solved in Eq. (34).

$$S_{21} = \frac{2V_c}{E_0} \tag{35}$$

The graph in Fig. 6 shows the explored frequency range within 100 MHz to 2 GHz in a horizontal logarithmic scale, while the vertical scale expresses $S_{21}$ in terms of dB. Theoretical data are provided by the curves with solid lines and experiments by dashed lines.

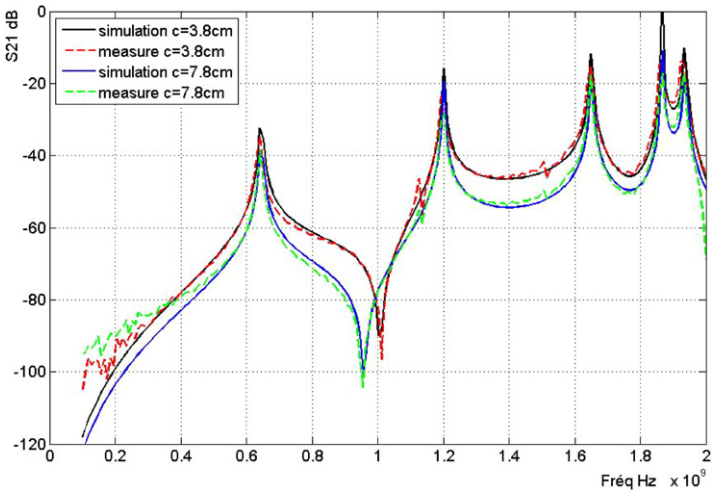


Fig. 6. $S_{21}$ parameter related to monopoles 1 and 2 from measurements and theory.

Table 1
Location of the resonance frequencies and the corresponding values of the coupling factors.

| Mode | Resonant frequency | $N_{mn}$ | $N'_{mn}$ |
|---|---|---|---|
| (1, 1) | 646 MHz | 1 | 0.705 |
| (3, 1) | 1.2 GHz | −1 | −0.705 |
| (1, 3) | 1.65 GHz | −1 | 0.713 |
| (5, 1) | 1.869 GHz | 1 | 0.705 |
| (3, 3) | 1.94 GHz | 1 | −0.713 |

Each peak of the curves in Fig. 6 deals with a 2D resonance of the cavity; we can notice that 25 resonators were considered in the computation including the combination of 25 2D $TM_{mn}$ appearing before the first 3D eigen mode. However, due to the location of the monopoles inside the cavity, 5 modes will be excited. The amplitude of the peak for the first 2D resonance corresponds exactly to the experiment, however, for the other resonances, we can observe a shift from the theory especially at peak amplitude of the curves. Some investigations showed that it is due to the sampling of the experimental and theoretical frequencies data. Increasing the frequency resolution shows a very good agreement between theory and measurements. From these results, we can conclude that the minimum amplitude acquired by $S_{21}$ is mainly influenced by the effect of direct coupling between the monopoles 1 and 2 and related to $M_{13}$ and $M_{31}$. Furthermore, when the height of the box is changed, the location of the minimum is somewhat moved.

Before extending the confrontation between measurements and theory to the final configuration with the voltage collected at monopole 3 output, the location of the frequencies of resonance in Fig. 6 and the corresponding values of $N_{mn}$ and $N'_{mn}$ coupling factors will be listed in Table 1.

However, due to the location of monopoles 1 and 2, among 25 available 2D modes, electromagnetic energy in the cavity is restricted to the above five modes as specified by $N_{mn}$ and $N'_{mn}$.

These experiments and computations were extended to the determination of $S_{21}$ parameter collected between monopole 1 and monopole 3, as shown in Fig. 7. Display scales and curves are the same as those used in Fig. 6. We can notice on this graph that the maximum and minimum amplitudes occurs at 2D resonance of the box, however, the curves are less sharp. This is due to the contribution of the coupling factor $Z_{CE}$ between the two long monopoles 2 and 3 with $h_2 = h_3 = 19$ cm, which acquire their first own resonance at frequency $f_0$ as shown in Eq. (36).

$$f_0 = \frac{v}{4h_3} = 394 \text{ MHz} \tag{36}$$

Consequently, other resonances of these wires occurring at frequencies $2f_0$, $3f_0$ and $4f_0$ are somewhat mixed with the resonance of the box itself, and it explains why the shape of the curves is changed. Nevertheless measurements curves are in agreement with theoretical curves.

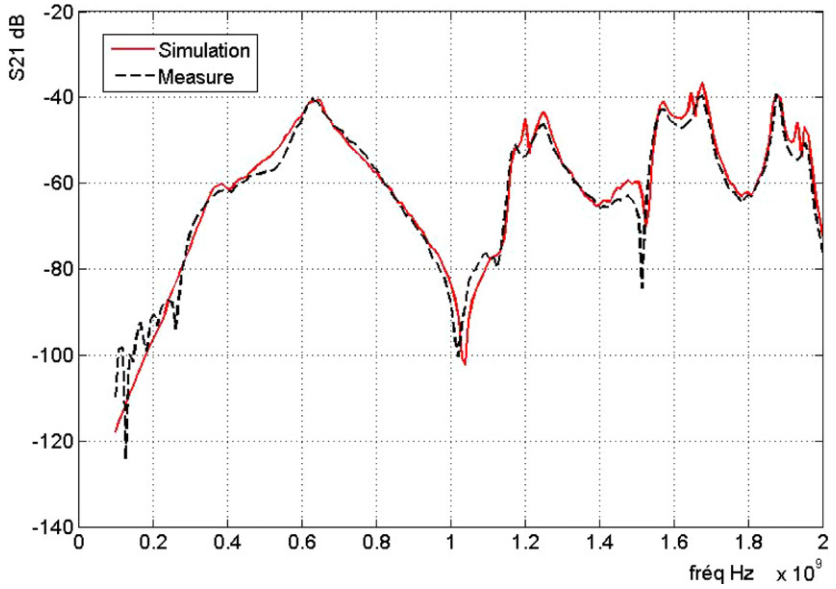


Fig. 7. $S_{21}$ parameter related to monopoles 1 and 3 from measurements and theory.

## 8. Conclusion

With the support of a flat rectangular shaped cavity, with a system of monopoles at both sides of the walls of the box coupled throughout, it has been shown that the transformation of the electromagnetic problem into a similar circuit diagram leads to the construction of a hyper matrix impedance. From a preliminary diagonal form of this matrix, neglecting all electromagnetic coupling, the main parameters relevant to various contributions such as the RF source connected to the system, or the resonance occurring at cavity level and the behaviors of monopoles, were characterized in terms of scalars and sub-matrices impedance. The second step was to include diagonal off parameters related to the various electromagnetic coupling as described in Section 5 of the paper. For convenience sake they were deduced from specific measurements carried out with a network analyzer. This hyper matrix impedance was solved by means of Kron's methodology and consequently related to the input emf vector and unknown mesh current vector. The response of the receiver connected to the dedicated out port of the system like the monopoles, was compared with measurements performed within a wide frequency range from 100 MHz to 2 GHz. From the comparison with the circuit computation, it was observed a good fitting especially when the cavity resonance and monopole resonance occur either separately or mixed together.

From this first test applied to EMC problem of large scale, we can conclude that the circuit approach seems to be efficient. Indeed, at first, we can assume that the theoretical prediction of the response of the concerned system using a full wave simulator requires a lot of computation time and amount of memory. Then, the use of theory circuit with the combination of topological diagram leads the subdivision of the computation work and consequently reduces the computation time dramatically. Furthermore, in a future study, this way may be combined with the tensorial formalism in order to make a dedicated software tool.

## Acknowledgements

This study was performed with the financial support of "Délégation Générale pour l'Armement".

## References

[1] C.E. Baum, Electromagnetic topology: A formal approach to the analysis and design of complex electronic systems, in: Interaction Notes 400, Kirtland, 1980; also in Proc. Zurich EMC Symp., 1981, pp. 209–214.

[2] J.P. Parmentier, Approche topologique pour l'étude des couplages électromagnétiques, ONERA Thèse soutenue à TELICE le 20 décembre 1991.

[3] O. Maurice, La compatibilité électromagnétique des systèmes complexes, éditions Lavoisier, 2007.
[4] M. Denis-Papin, A. Kaufmann, Cours de calcul TENSORIEL, éditions Albin Michel, 1966.
[5] G. Kron, Equivalent circuit of the field equations of Maxwell-I, in: Proceedings of the I.R.E., May 1944, pp. 289–299.
[6] M. Cauterman, Du fonctionnement des chambres réverbérantes, Séminaire de Recherche DRE et TELICE, Lille, juillet 2005.
[7] S. Bazzoli, S. Baranowski, M. Cauterman, B. Démoulin, Simulation d'une cavité 2D par l'assemblage de résonateurs RLC, in : 13e colloque International et Exposition sur la Compatibilité Electromagnétique (CEM 2006), St Malo, avril 2006, pp. 144–145.
[8] F.M. Tesche, M.V. Lanoz, T. Karlsson, EMC Analysis Methods and Computational Models, John Wiley & Sons, Inc., 1996, p. 145.